Analytical and Bioanalytical Chemistry (2019) 411:147–156
https://doi.org/10.1007/s00216-018-1436-5

PAPER IN FOREFRONT

Nanoparticle microarray for high-throughput microbiome metabolomics using matrix-assisted laser desorption ionization mass spectrometry

Rebecca L. Hansen[1] · Maria Emilia Dueñas[1] · Torey Looft[2] · Young Jin Lee[1]

Received: 3 September 2018 / Revised: 6 October 2018 / Accepted: 17 October 2018 / Published online: 30 October 2018

Abstract

A high-throughput matrix-assisted laser desorption/ionization mass spectrometry (MALDI)-MS-based metabolomics platform was developed using a pre-fabricated microarray of nanoparticles and organic matrices. Selected organic matrices, inorganic nanoparticle (NP) suspensions, and sputter coated metal NPs, as well as various additives, were tested for metabolomics analysis of the turkey gut microbiome. Four NPs and one organic matrix were selected as the optimal matrix set: α-cyano-4-hydroycinnamic acid, Fe_3O_4 and Au NPs in positive ion mode with 10 mM sodium acetate, and Cu and Ag NPs in negative ion mode with no additive. Using this set of five matrices, over two thousand unique metabolite features were reproducibly detected across intestinal samples from turkeys fed a diet amended with therapeutic or sub-therapeutic antibiotics (200 g/ton or 50 g/ton bacitracin methylene disalicylate (BMD), respectively), or non-amended feed. Among the thousands of unique features, 56 of them were chemically identified using MALDI-MS/MS, with the help of in-parallel liquid chromatography (LC)-MS/MS analysis. Lastly, as a proof of concept application, this protocol was applied to 52 turkey cecal samples at three different time points from the antibiotic feed trial. Statistical analysis indicated variations in the metabolome of turkeys with different ages or treatments.

Keywords Metabolomics · MALDI · Mass spectrometry · Nanoparticles · Turkey · Microbiome · High-throughput

Introduction

Mass spectrometry (MS)–based metabolomics research has seen exponential growth in the past decade [1]. Most MS-based metabolomics experiments make use of liquid chromatography-electrospray ionization (LC-ESI). While chromatographic separation provides comprehensive analysis of a complex mixture, this technique requires long data acquisition times, thus making large-scale analysis challenging due to limitations in time and cost [2–4]. Matrix-assisted laser desorption/ionization (MALDI)-MS has been suggested as an alternative to ESI-MS for high-throughput metabolomics analysis [5, 6]; however, its application has been limited due to (i) interference from matrix peaks in the low-mass range, (ii) difficulty in compound identification because of the lack of chromatographic separation, and (iii) limited metabolite coverage depending on the choice of matrix. To overcome the first limitation, matrices with no or minimum interferences have been developed, such as nanoparticles (NPs) [7] or basic matrices in negative mode [8, 9], while high-resolution mass spectrometry (HRMS) can partially overcome the lack of separation.

The recent evolution of NPs as MALDI matrices has significantly contributed to small molecule analysis by MALDI-MS [10]. Most NPs have UV absorption and can be homogeneously applied, which is useful for imaging applications and to minimize spot-to-spot variation. They are especially useful for the small molecule analysis due to their no or low matrix background peaks [11]. Recently, our group has performed a large-scale systematic LDI-MS screening of 13 different NPs,

Rebecca L. Hansen and Maria Emilia Dueñas contributed equally to this work.

Electronic supplementary material The online version of this article (https://doi.org/10.1007/s00216-018-1436-5) contains supplementary material, which is available to authorized users.

✉ Young Jin Lee
yjlee@iastate.edu

[1] Department of Chemistry, Iowa State University, Ames, IA 50011, USA

[2] United States Department of Agriculture, National Animal Disease Center, Ames, IA 50010, USA

including metal oxide NPs, carbon-based NPs, and metal NPs, for the analysis of two dozen small metabolite molecules [12]. As capping agents were not used for these NPs to avoid contamination from these organic compounds, aggregation of some NPs, especially metals, caused significant loss of ion signals. To eliminate this problem, physical vapor deposition (PVD), commonly known as sputter coating, has been recently used as a means to create NPs in situ, as demonstrated previously for Au, Ag, and Pt [13–15].

Antibiotics are essential to animal health and production. Sub-therapeutic levels of antibiotics have been commonly utilized for growth promotion, but starting in 2017, FDA guidance 209 restricted the off-label and feed-efficiency usage of antibiotics determined to be important for human health [16]. Although antibiotics have long been known to disrupt the gastrointestinal microbiome, the impact on the bacterial population (microbiota) and the metabolomic interplay is poorly understood [17–19]. The relationship between the microbiota and its metabolome is a dynamic system with tremendous individual and temporal variations, which may not be revealed by small sets of data. Large-scale studies are necessary to find the correlation between microbiota membership and the gut metabolome in each individual animal. However, the lack of a high-throughput low-cost metabolomics platform is a serious bottleneck toward that end.

Here, we propose a high-throughput MALDI-MS-based metabolomics approach using a set of nanoparticles or matrices in a microarray format. Due to differences in analyte selectivity between matrices, a carefully chosen set of matrices can effectively enhance metabolite coverage, thus allowing diverse classes of small molecule metabolites to be analyzed. While it is impossible to achieve a metabolomic profile as comprehensive as LC-MS-based metabolomics, we hypothesize it is possible to grasp some important features with this approach. In the current study, this platform was optimized and then, as a proof of concept, applied to 52 turkey gut microbiome samples treated with therapeutic or sub-therapeutic dosages of the antibiotic bacitracin methylene disalicylate (BMD).

Materials and methods

Materials

Isopropyl alcohol (IPA), methanol (MeOH), water (H_2O), acetonitrile (ACN), piperidine (99%), triethylamine (> 99%), ammonium hydroxide, formic acid (> 95%), sodium acetate (> 99%), and trifluoroacetic acid (TFA, 99%) were purchased from Sigma-Aldrich (St. Louis, MO, USA); solvents were purchased in CHROMASOLV LC-MS or Plus grade. Organic matrices were purchased from Sigma-Aldrich (St. Louis, MO, USA): 1,5-diaminonaphthalene (DAN, 97%), 2,5-dihydroxybenzoic acid (DHB, 98%), α-cyano-4-hydroxycinnamic acid (CHCA, 99%), and 9-aminoacridine (9AA, 98%) hydrochloride hydrate. The basic form of 9AA was prepared by dissolving the hydrochloride salt in boiling water and adding excess sodium hydroxide to precipitate the free base. The product was isolated by filtration and rinsed several times with cold water, then dried under vacuum. Aluminum-doped zinc oxide (AZO; zinc oxide NPs doped with 2 wt% aluminum oxide, 99.99%, 15 nm) was purchased from US Research Nanomaterials, Inc. (Houston, TX, USA). Iron oxide NPs (Fe_3O_4, 11 nm, no organic capping) and titanium dioxide NPs (TiO_2) were synthesized as previously described [12]. Characterization of these NPs can also be found in the supplementary information of the work by Yagnik et al. [12]. The sputter targets were purchased from Ted Pella, Inc. (Redding, CA, USA): silver (99.99%), gold (99.99%), titanium (99.6%), and copper (99.99%). The μFocus LDI plates (5 × 16 circles, 600 μm) were purchased from Hudson Surface Technology (Old Tappan, NJ, USA).

Animal experiment and metabolite extraction

All animal experiments were performed at the National Animal Disease Center (NADC), USDA, Ames, IA, USA, following the ethical guidelines set by the Institutional Animal Care and Use Committee (IACUC) using the approved protocol ARS-2869. As a part of a larger animal microbiome study (manuscript submitted), 240 day-of-hatch Nicholas turkey poults (Valley of the Moon Hatchery, Osceola, IA) were obtained and allowed to comingle and acclimate for 2 weeks. At 2 weeks of age, birds were randomly separated into one of three rooms to begin antibiotic treatment of 50 g/ton feed or 200 g/ton feed BMD for sub-therapeutic or therapeutic treatments, respectively, or non-medicated diet. Sub-therapeutic BMD was administered continuously for 11 weeks. Therapeutic BMD was given for 5 weeks, followed by reduction to sub-therapeutic concentration for 6 weeks. Ten turkeys were sampled from each group after euthanasia, taken at 7, 35, and 78 after the start of the antibiotic therapy. Two hundred milligrams of cecal contents from each bird was flash frozen in liquid nitrogen for metabolomics analysis. Lyophilized cecal contents (~ 5 mg) were placed in a 1.5-mL centrifuge tube and then suspended in 1.0 mL of extraction solvent with internal standards (5 μl of 10 mg/mL jasmonic acid, 5 μl of 10 mg/mL ^{13}C-ribitol, 495 μL H_2O, 495 μL MeOH). Extraction proceeded with 10 min of vortexing (1400 rpm), followed by centrifuging for 10 min (12,000 rpm). The hydrophilic supernatant was transferred to a new 1.5-mL centrifuge tube. The samples were dried under vacuum and re-suspended to a final concentration of 1 mg/mL with ACN:H_2O (50:50).

Workflow for LDI-MS analysis

The overall workflow for the experiments and an example of the microarrays used in the initial optimization are illustrated

in Fig. 1. Organic or NP matrix solutions were prepared by dissolving or suspending in IPA at a concentration of 10 mM. Organic matrices were vortexed for ~1 min and NP matrix solutions were sonicated for ~1 h before spotting. For the microarrays made from organic matrix solutions or NP suspensions, 2 μL of matrix solution, followed by 2 μL turkey cecal contents extraction and 2 μL additive solution (optional), was spotted on a μFocus LDI plate (Hudson Surface Technology; Old Tappan, NJ, USA). All of the solutions were spotted on a μFocus LDI plate pre-heated to 45 °C to ensure uniform deposition. Spots were completely dried before the next solution was spotted. CHCA, DHB, and Fe_3O_4 were tested for positive mode, and 9AA, DAN, and AZO were tested for negative mode. TiO_2 was used for both ion modes.

For the metal NP microarrays deposited through PVD, 2 μL of cecal extract was spotted first, followed by 2 μL of additive solution (optional), and then metal NPs were sputter coated using a Cressington 108Auto (Ted Pella). The portion of the plate that was not to be sputter coated was covered using a glass slide. The optimized sputter times are 5, 10, 20, and 40 s for Ag, Au, Ti, and Cu, respectively. Both positive and negative modes were used for all the sputter coated metals.

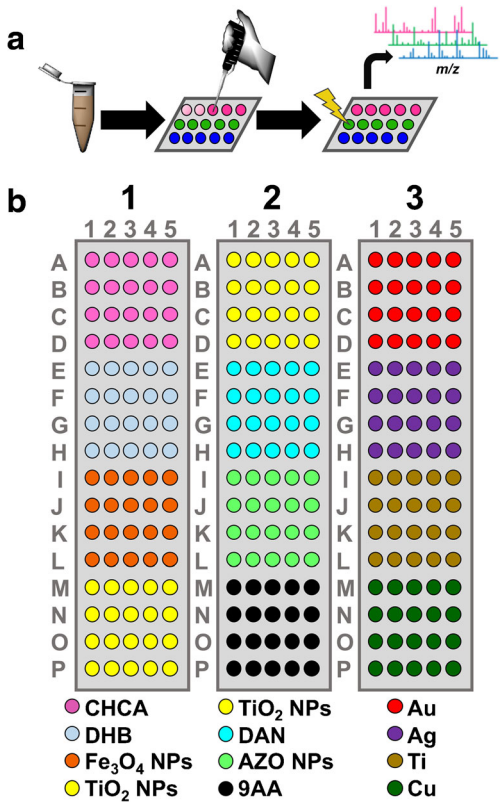

Fig. 1 **a** The overall workflow of matrix microarray experiment. An extraction was conducted on the turkey cecal sample, followed by spotting (or sputtering) the matrix, extract, and additives onto the μFocus LDI plate. High-resolution Orbitrap scans were acquired and the data was analyzed using MSiReader and Xcalibur. **b** Examples of matrix spotted and metal sputtered coated microarrays. For prefabricated pipet spotted microarray (plates 1 and 2, in positive and negative ion mode, respectively), 2 μL of matrix, followed by 2 μL turkey cecum extract sample, and 2 μL additive were spotted on a LDI plate. For PVD microarray (plate 3), 2 μL turkey cecum extract sample was spotted first, followed by 2 μL of additive, and then the metal was sputtered

In order to improve the detection of unique features, three different additives were tested in each polarity. For positive ion mode, 0.1% TFA (*v*/*v*), 0.1% formic acid (*v*/*v*), and 10 mM sodium acetate were used. For negative ion mode, 1% piperidine (*v*/*v*), 1% triethylamine (*v*/*v*), and 10 mM ammonium formate were used for this test. The additives were compared to see which offered the most unique features.

Mass spectrometry analysis

A linear ion-trap Orbitrap mass spectrometer with a MALDI ion source (MALDI LTQ-Orbitrap Discovery; Thermo Scientific, San Jose, CA, USA) was used to acquire data in imaging mode for each circle in the microarray, approximately 300–375 pixels per circle. The instrument was modified to use an external frequency-tripled, diode-pumped Nd:YAG laser operating at 355 nm and 60 Hz (UVFQ; Elforlight Ltd., Daventry, UK). Data was collected using a 150-μm raster step size and a ~30-μm laser spot size. Laser pulse energies were optimized individually for each matrix. MSiReader [20] and Xcalibur (ThermoFisher Scientific) were used to define imaging parameters and to acquire data, respectively. Mass spectra were acquired with ten laser shots per spectrum using an Orbitrap mass analyzer (resolution of 30,000 at a mass to charge ratio (*m*/*z*) of 400) for an *m*/*z* scan range of 50–1000.

Estimation of potential metabolites based on accurate mass

The total number of potentially identifiable metabolites (i.e., unique features) was estimated based solely on accurate mass. The mass spectra over the entire circle were averaged and all *m*/*z* values and their ion intensities were exported as *.csv* files using MSiReader. Two levels of filtering were applied to extract only those *m*/*z* values that are meaningful. In the first filtering, any *m*/*z* values at noise level with an absolute intensity below 500 (signal-to-noise ratio of 20) were removed. In the second filtering, matrix and contamination peaks (background outside the region of interest), as well as 13 carbon isotopes, alkali metal adducts in positive mode, and a water loss in negative mode, were removed using an in-house Python script within a 5-ppm tolerance. MS images were then generated for all remaining *m*/*z* values using MSiReader and inspected to ensure they were not also present in the background. This final mass list was compared to the compound list identified by Metabolon using an LC-MS/MS approach (see the "LC-MS/MS-based identification of turkey gut microbiome" section). For the matching features based on accurate mass within 5 ppm mass tolerance, MS/MS was

performed using the ion-trap analyzer using an isolation width of 2.0 Da. The collision energies were individually optimized for each metabolite. MetFrag [21] and CFM-ID [22] were used to aide metabolite identification.

LC-MS/MS-based identification of turkey gut microbiome

Metabolomics analysis was performed by Metabolon (Morrisville, NC) for a selected set of turkey gut microbiome samples (manuscript submitted). In short, proteins were precipitated with methanol under vigorous shaking for 2 min (Glen Mills GenoGrinder 2000) followed by centrifugation. The resulting extract was divided into five fractions: two for analysis by two separate reverse phase (RP)/ultra-performance liquid chromatography (UPLC)-MS/MS methods in positive ion mode electrospray ionization (ESI), one for analysis by RP/UPLC-MS/MS with negative ion mode ESI, one for analysis by HILIC/UPLC-MS/MS with negative ion mode ESI, and one sample was reserved for backup. All methods utilized a Waters ACQUITY UPLC and a Thermo Scientific Q-Exactive HRMS. Compounds were identified with the Metabolon library based on authenticated standards that contain the retention time/index (RI), mass to charge ratio (*m/z*), and chromatographic data (including MS/MS spectral data) for all molecules present in the library.

Results and discussion

Finding the optimal experimental conditions for development of nanoparticle microarray

The overall workflow is illustrated in Fig. 1a. Samples were directly deposited on a pre-spotted NP or matrix microarray, which can be done in a high-throughput manner, especially using a multichannel pipettor or robotic autosampler. The microarray was prepared using a μFocus MALDI plate and matrix deposition was done on a heated plate to reduce signal variation due to the inhomogeneity of matrix crystals. The surface of μFocus MALDI plate is hydrophobic, except for an array of small circles with hydrophilic surfaces, so that samples in aqueous solutions can be focused onto small areas. This study focused on utilizing various NPs as MALDI matrices, as they are particularly useful in high-throughput small molecule analysis due to their no or low matrix background peaks as well as homogeneous application with minimal signal variation [12]. Then, after the microarrays were prepared, MALDI-MS data acquisition was performed in as fast as a few minutes for a set of matrices, and hundreds of samples can be run in a single day without manual interruption using batch mode operation.

Optimization of the microarrays was performed using cecal samples from several pooled non-medicated, 93-day-old turkeys. Different matrices and additives were tested to find conditions that yielded the most comprehensive coverage of metabolites of interest. Three NPs from our previous study (Fe_3O_4, AZO, TiO_2) [12], four traditional organic matrices (CHCA, DHB, 9AA, DAN), and four PVD metals (Ag, Au, Ti, Pt) were selected in this preliminary study. Three different additives were tested in each polarity in order to improve the ionization efficiencies of unique features. For positive ion mode, 0.1% TFA, 0.1% formic acid, and 10 mM sodium acetate were used. For negative ion mode, 1% piperidine, 1% trimethylamine, and 10 mM ammonium formate were used for this test.

Venn diagrams comparing the number of unique features detected when using different additives in negative and positive ion modes can be found in Electronic Supplementary Material (ESM) Fig. S1. Unique features are defined as having a signal-to-noise ratio of at least 20, and matrix peaks, known contaminations, 13-carbon isotopes, and multiple adducts (see experimental section for the details) were excluded. As can be seen in ESM Fig. S1, there was little benefit of using additives in negative mode. However, in positive ion mode, the use of 10 mM sodium acetate significantly increased the number of unique features. For example, Fe_3O_4 and CHCA show ~ 2 and ~ 1.5 times more features, respectively, when sodium acetate was used, compared to no additive, due to the efficient formation of sodium ion adducts. Figure 2 shows Venn diagrams summarizing the number of unique features for various matrices with 10 mM sodium acetate in positive mode and with no additive in negative mode. In total, over one thousand unique features are identified in each polarity. However, it would take too long for data acquisition if all eight matrices were used in each polarity.

Out of eight matrices in each polarity, the five most effective matrices were chosen from Fig. 2 in terms of total coverage: Fe_3O_4, CHCA, and Au in positive ion mode, and Cu and Ag in negative ion mode. In positive mode, Ag has a slightly higher number of unique features than Au; however, many of these overlap with those from Fe_3O_4 (comparison not shown). Additionally, Ag in positive mode results in silver adducts and clusters which can complicate the spectrum. In negative mode, Au has the same number of unique features as Cu, but Cu was selected as many of the Au features overlap with Ag. Figure 3a compares mass spectra from the pooled control sample among the five matrices/NPs represented in a barcode-like pattern to facilitate quick and easy comparison of the distribution of features. The overlap is minimal in the metabolite coverage for each matrix/NP. Cu and Ag have the greatest coverage in the mass range of *m/z* 100–300, due to the tendency of metabolites effectively ionized in negative mode to have lower masses, while Fe_3O_4 provides comprehensive coverage over the entire mass range of *m/z* 100–500. Overall,

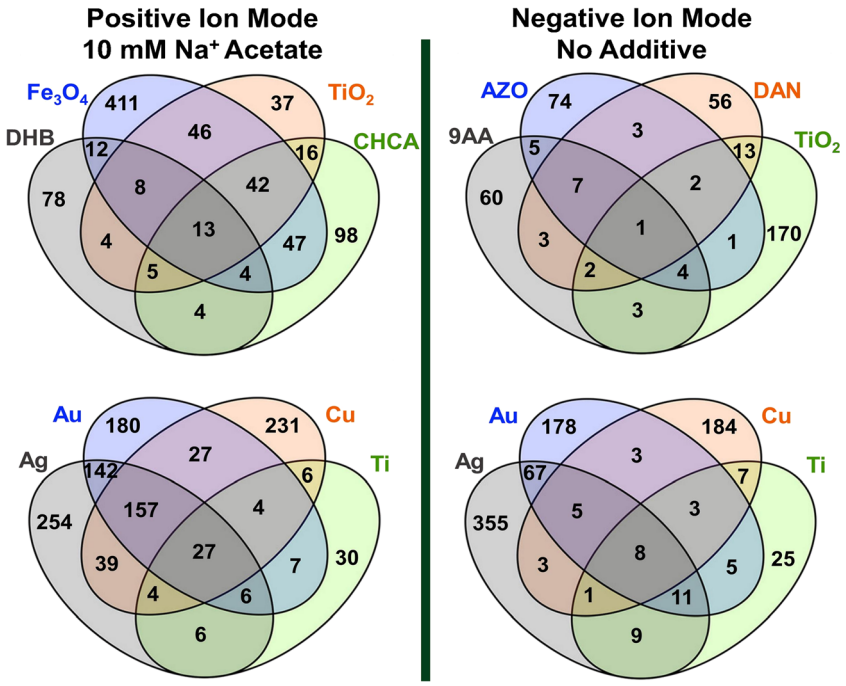

Fig. 2 Venn diagrams displaying the number of unique features observed when comparing different matrices in positive and negative ion mode. The number of unique compounds shown is after the removal of adducts

this data suggests that these five matrices/NPs can be used to detect a wide range of metabolites in the gut microbiome.

Proof of concept application using turkey microbiome samples

The optimal experimental conditions were then applied to cecal samples collected from 93-day-old turkeys that were either non-medicated, or treated with sub-therapeutic antibiotics, or therapeutic antibiotics. Figure 3b compares the total number of unique features for each sample type combined from all five matrices/NPs that were detected consistently in all three biological replicates. As a particular metabolite can be detected with multiple matrices, the reported total numbers of features in each sample type have been carefully screened to remove any duplicate features. Over 1000 unique metabolite features were detected in each sample type, and several hundred of them are unique to each, suggesting the potential of this approach for covering a diverse range of metabolites. A total of approximately 2100 unique features are detected combining all three sample types. The distribution of the total detected features from each sample type for each of the matrices/NPs used is shown in ESM Fig. S2.

Identifying all these compounds is not feasible, especially without chromatographic separation and standard analysis. Therefore, we focused our analysis to a handful of compounds that were also detected with in-parallel UPLC-MS/MS-based metabolomics performed by Metabolon (metabolon.com; a separate manuscript in preparation) and that were confirmed through MALDI-MS/MS. Metabolon performed extensive metabolomics profiling using four different UPLC-MS/MS runs (two in positive and two in negative mode, optimized

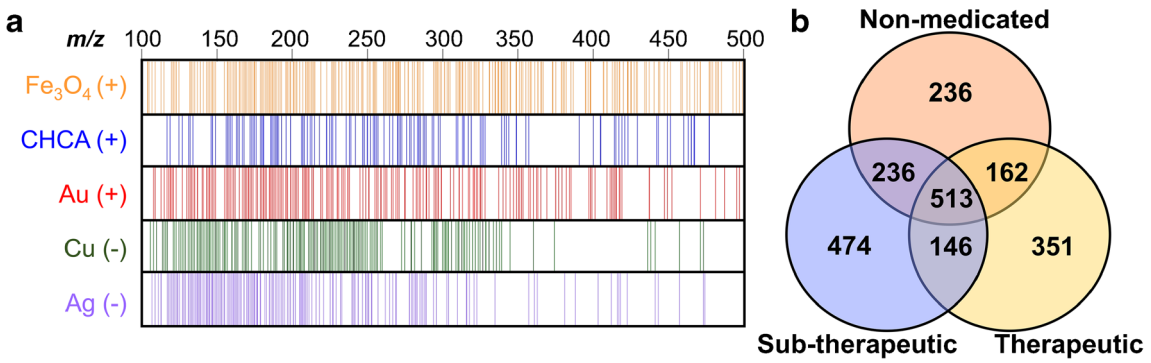

Fig. 3 **a** Microarray MALDI-MS results of turkey microbiome for optimal matrices, shown in a barcode-like pattern. **b** Venn diagram displaying the total number of unique features observed across in all five matrices, using the optimized experimental conditions

for hydrophilic and hydrophobic compounds each) and compared these to over 3000 entries in an in-house standard library. Selected samples from the 7, 35, and 78 days post-treatment time points for each of non-medicated, sub-therapeutic treated, and therapeutic treated were analyzed ($n = 6$ per condition). A total of 712 unique metabolites were chemically identified in the Metabolon study, while thousands more unique features were unidentified. Among those identified in the Metabolon data, 96 match features shown in Fig. 3b within 5 ppm mass tolerance. MALDI-MS/MS was performed for each of the 96 matching compounds, and 56 of them were confirmed to match with the Metabolon-identified chemical structures. The list of identified compounds is summarized in ESM Table S1 along with fragment ions from MS/MS. Some metabolites have mass differences that are less than what can be isolated by the ion trap. In that case, they are simultaneously fragmented and the combination of exact mass and MS/MS information was utilized to identify the metabolites. Assignments were made based on the presence of (i) a unique precursor ion in the MS spectrum and (ii) at least one corresponding fragment in the MS/MS spectrum. The results of the metabolomics study performed by Metabolon are beyond the scope of the current work and will be presented in a separate publication.

Mid-throughput screening comparing antibiotic treatments

Previous studies using MALDI-MS-based metabolomics have targeted specific metabolites and thus have been limited in scope mostly due to low metabolite coverage, resulting from the lack of chromatographic separation [6, 23–25]. Here, we use MALDI MS combined with a microarray platform for metabolomics analysis to compare the gut microbiome of different antibiotic treated turkeys. As a proof of concept experiment demonstrating that a nanoparticle microarray–based MALDI-MS platform can be used for a large-scale high-throughput analysis, this method was applied to a total of 52 turkey gut microbiome samples from three different antibiotic treatment groups (therapeutic, sub-therapeutic, and non-medicated). After 2 weeks of co-mingling, young turkeys were separated into three treatment groups, and samples were collected at three time periods (7, 35, and 78 days) after the start of treatment ($n = 5$ or 6 for each condition). We used a microarray MALDI plate with a spot size of 600 μm, and data was collected for about 5 minutes per spot. The total data acquisition time was 2.7 days in the current study (52 samples × 5 matrix × 3 analytical replicates × 5 min), but it could be shorted to a half-day for a 1-min data acquisition time using a MALDI plate with smaller focus size. The same number of experiments would take 1or 2 weeks using LC-MS–based metabolomics. Additionally, to save data acquisition time, analytical replicates are often ignored as there are multiple biological replicates; however, as discussed below, each individual animal is different and therefore shows slightly different metabolomic profiles, presumably due to their different microbiota membership.

The signal intensities for the compounds listed in ESM Table S1 were extracted for each cecal sample and then uploaded to MetaboAnalyst (http://metaboanalyst.ca) [26] for statistical analysis, after averaging over analytical replicates and normalized to internal standard: the sum of ^{13}C-ribitol adducts in positive mode (*m/z* 154.080, 176.062, and 192.036 for $[M+H]^+$, $[M+Na]^+$, and $[M+K]^+$, respectively) or jasmonic acid in negative mode (*m/z* 209.118 for $[M-H]^-$). Figure 4a shows three-dimensional partial

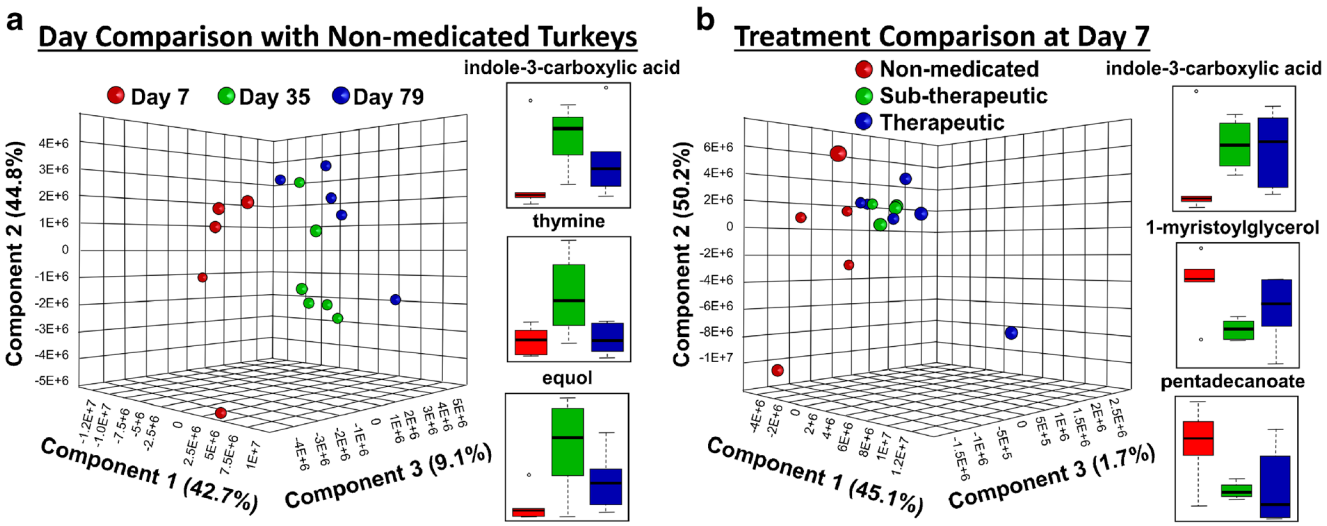

Fig. 4 Three-dimensional partial least squares discriminant analysis (PLSDA) and box and whisker plots for selected metabolites for **a** day comparison with non-medicated turkeys and **b** treatment comparison at day 7

least squares discriminant analysis (PLSDA) for non-medicated turkeys from the three studied time points as well as box and whisker plots for selected differentiating metabolites. Moderate separation is clear between different groups, especially in the three-dimensional space. Metabolites shown in Fig. 4a (indole-3-carboxylic acid, thymine, equol) have significant increases in day 35, compared to day 7, and then stabilize to lower levels at day 78. It is well known that poultry microbiota changes in membership over time and with host age, so these differences are likely due to aging [27, 28]. Figure 4b shows PLSDA of the treatment comparison at the day 7 time point, which also shows moderate but clear separation between groups as well as box and whisker plots. Indole-3-carboxylic acid shows a dramatic increase for therapeutic and sub-therapeutic treatments compared to non-medicated birds, whereas 1-myristoylglycerol and pentadecanoate are decreased, indicating significant changes in gut microbiome metabolites during antibiotic usage. Fatty acids are known to be involved with antibiotics [29, 30] and are constituents of bacterial membranes [31], particularly odd-chain fatty acids like pentadecanoate. Indole-3-carboxylic acid has been shown to play a role in intra- and inter-kingdom signaling [32–34] and regulates expression of genes involved in a variety of processes including metabolism and stress [34]. Additionally, microbial-derived indole metabolites have been shown to be important drivers of intestinal health, binding with the host aryl hydrocarbon receptor, modulating immune responses along the mucosa [35]. Data like these may help identify bacterial functions that can be targeted to improve animal health. In all cases, the trend of these metabolites is in good agreement with the data provided by Metabolon (not shown).

Statistical analysis shows relatively moderate separation, which is attributed to high variation among the individual turkeys. Figure 5 shows an example demonstrating that biological variation is much greater than analytical variation for these metabolites. Selected metabolites from four day 7 non-mediated turkeys which were raised in the same room are compared to show the biological and analytical variations. The standard deviations for each metabolite (i.e., the analytical variation) are very narrow, whereas the differences between the mean values for each animal (i.e., the biological variation) are quite large, especially for certain metabolites. This is typical in animal studies with outbred animals. We hypothesize this is likely due to the variability in the microbiota composition and host genetics, between turkeys. 16S rRNA gene sequence analysis has identified microbiota membership and compositional differences between treatment groups, as well as inter-group variability (data not shown). The correlation between members of the microbiota and metabolites within the metabolome is currently under investigation.

Conclusions

The use of microarray technology is a common analytical platform for other types of analyses, most notably DNA or RNA [36–38]. In the field of mass spectrometry, surface-enhanced laser desorption (SELDI), a variation of MALDI-MS, was developed in the early 1990s for protein analyses [39]. In this technique, biological samples such as blood or urine are spotted onto special microarray surfaces which bind certain proteins whereas any others are washed away. Various surfaces have been used for this purpose, mostly based on chromatographic interactions, although chemically modified reactive surfaces can also be used. This technology has been commercialized by Biorad (http://www.bio-rad.com). SELDI-MS, however, works only for large proteins and there has been no microarray MALDI-MS platform for small metabolite analysis.

In this study, we developed and optimized a pre-fabricated microarray for high-throughput metabolomics analysis. It was determined that the addition of sodium acetate yielded more features in positive mode data than with no additive. Out of an initial eight matrices/NPs in each polarity, a total of five

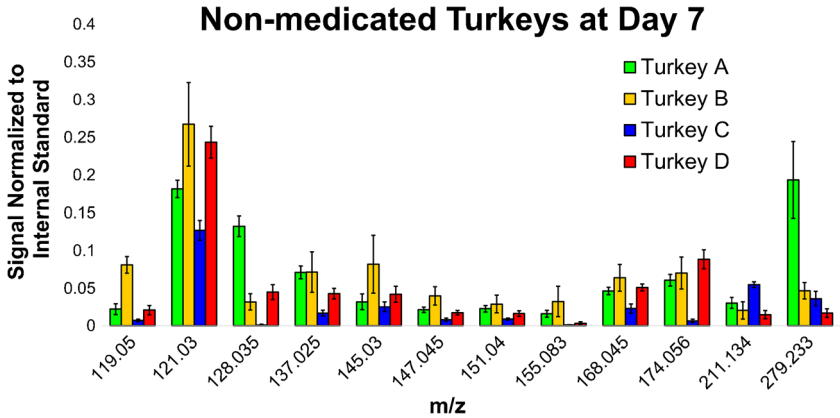

Fig. 5 Representative metabolites signals of four turkeys (**a**–**d**) of the same age raised in the same room

matrices/NPs were selected for inclusion in the final NP microarray platform: Fe_3O_4, CHCA, and Au in positive ion mode, and Ag and Cu in negative ion mode. We were able to successfully apply our microarray platform to compare a large sample set of non-medicated, sub-therapeutic treated, or therapeutic treated turkey cecal samples 7, 35, and 78 days after the start of antibiotic treatment with our optimized conditions. We detected thousands of unique metabolite features and monitored their changes over time or with antibiotic treatment.

The identification of thousands of unique features is the current bottleneck in this approach. However, we demonstrated it could be partially mitigated through in-parallel LC-MS/MS metabolomics analysis and MALDI-MS/MS of selected metabolites. While the traditional chromatography-based method gives more comprehensive coverage, the analysis of all samples in a large-scale study with this method would be costly and require extensive data acquisition time. Our high-throughput microarray technology, however, can be used to quickly acquire the large data sets needed for the study of a dynamic system, such as the turkey gut microbiome, and, as shown here, can be used in combination with a chromatographic-based study to enable high-throughput metabolomics experiments.

Funding information This work was funded by the United States Department of Agriculture-National Institute of Food and Agriculture (USDA-NIFA).

Compliance with ethical standards

All animal experiments were performed at the National Animal Disease Center (NADC), USDA, Ames, IA, USA, following the ethical guidelines set by the Institutional Animal Care and Use Committee (IACUC) using the approved protocol ARS-2869.

Conflict of interest The authors declare that they have no conflict of interest.

References

1. Dettmer K, Aronov PA, Hammock BD. Mass spectrometry-based metabolomics. Mass Spectrom Rev. 2007;26(1):51–78. https://doi.org/10.1002/mas.20108.
2. Wikoff WR, Anfora AT, Liu J, Schultz PG, Lesley SA, Peters EC, et al. Metabolomics analysis reveals large effects of gut microflora on mammalian blood metabolites. Proc Natl Acad Sci U S A. 2009;106(10):3698–703. https://doi.org/10.1073/pnas.0812874106.
3. Aretz I, Meierhofer D. Advantages and pitfalls of mass spectrometry based metabolome profiling in systems biology. Int J Mol Sci. 2016;17(5). https://doi.org/10.3390/ijms17050632.
4. Dunn WB, Erban A, Weber RJM, Creek DJ, Brown M, Breitling R, et al. Mass appeal: metabolite identification in mass spectrometry-focused untargeted metabolomics. Metabolomics. 2013;9(1):44–66. https://doi.org/10.1007/s11306-012-0434-4.
5. Fagerer SR, Nielsen S, Ibáñez A, Zenobi R. Matrix-assisted laser desorption/ionization matrices for negative mode metabolomics. Eur J Mass Spectrom. 2013;19(1):39–47. https://doi.org/10.1255/ejms.1209.
6. Wang J-N, Zhou Y, Zhu T-Y, Wang X, Guo Y-L. Prediction of acute cellular renal allograft rejection by urinary metabolomics using MALDI-FTMS. J Proteome Res. 2008;7(8):3597–601. https://doi.org/10.1021/pr800092f.
7. Korte AR, Stopka SA, Morris N, Razunguzwa T, Vertes A. Large-scale metabolite analysis of standards and human serum by laser desorption ionization mass spectrometry from silicon nanopost arrays. Anal Chem. 2016;88(18):8989–96. https://doi.org/10.1021/acs.analchem.6b01186.
8. Korte AR, Lee YJ. MALDI-MS analysis and imaging of small molecule metabolites with 1, 5-diaminonaphthalene (DAN). J Mass Spectrom. 2014;49(8):737–41.
9. Shroff R, Svatoš A. Proton sponge: a novel and versatile MALDI matrix for the analysis of metabolites using mass spectrometry. Anal Chem. 2009;81(19):7954–9. https://doi.org/10.1021/ac901048z.
10. Lu M, Yang X, Yang Y, Qin P, Wu X, Cai Z. Nanomaterials as assisted matrix of laser desorption/ionization time-of-flight mass spectrometry for the analysis of small molecules. Nanomaterials. 2017;7(4):87. https://doi.org/10.3390/nano7040087.
11. Chiang C-K, Chen W-T, Chang H-T. Nanoparticle-based mass spectrometry for the analysis of biomolecules. Chem Soc Rev. 2011;40(3):1269–81. https://doi.org/10.1039/c0cs00050g.
12. Yagnik GB, Hansen RL, Korte AR, Reichert MD, Vela J, Lee YJ. Large scale nanoparticle screening for small molecule analysis in laser desorption ionization mass spectrometry. Anal Chem. 2016;88(18):8926–30. https://doi.org/10.1021/acs.analchem.6b02732.
13. Kawasaki H, Ozawa T, Hisatomi H, Arakawa R. Platinum vapor deposition surface-assisted laser desorption/ionization for imaging mass spectrometry of small molecules. Rapid Commun Mass Spectrom. 2012;26(16):1849–58. https://doi.org/10.1002/rcm.6301.
14. Dufresne M, Thomas A, Breault-Turcot J, Masson J-F, Chaurand P. Silver-assisted laser desorption ionization for high spatial resolution imaging mass spectrometry of olefins from thin tissue sections. Anal Chem. 2013;85(6):3318–24. https://doi.org/10.1021/ac3037415.
15. Dufresne M, Masson J-F, Chaurand P. Sodium-doped gold-assisted laser desorption ionization for enhanced imaging mass spectrometry of triacylglycerols from thin tissue sections. Anal Chem. 2016;88(11):6018–25. https://doi.org/10.1021/acs.analchem.6b01141.
16. Medicine FaDACfV (2012) The judicious use of medically important antimicrobial drugs in food-producing animals. Author, Rockville, MD.
17. Hernandez E, Bargiela R, Diez MS, Friedrichs A, Perez-Cobas AE, Gosalbes MJ. Functional consequences of microbial shifts in the human gastrointestinal tract linked to antibiotic treatment and obesity. Gut Microbes. 2013;4. https://doi.org/10.4161/gmic.25321.
18. Vernocchi P, Del Chierico F, Putignani L. Gut microbiota profiling: metabolomics based approach to unravel compounds affecting human health. Front Microbiol. 2016;7:1144. https://doi.org/10.3389/fmicb.2016.01144.

19. Yan S, Huang J, Chen Z, Jiang Z, Li X, Chen Z. Metabolomics in gut microbiota: applications and challenges. Sci Bull. 2016;61(15): 1151–3. https://doi.org/10.1007/s11434-016-1142-7.
20. Robichaud G, Garrard KP, Barry JA, Muddiman DC. MSiReader: an open-source Interface to view and analyze high resolving power MS imaging files on Matlab platform. J Am Soc Mass Spectrom. 2013;24(5):718–21. https://doi.org/10.1007/s13361-013-0607-z.
21. Ruttkies C, Schymanski EL, Wolf S, Hollender J, Neumann S. MetFrag relaunched: incorporating strategies beyond in silico fragmentation. J Cheminform. 2016;8(1):3. https://doi.org/10.1186/s13321-016-0115-9.
22. Allen F, Pon A, Wilson M, Greiner R, Wishart D. CFM-ID: a web server for annotation, spectrum prediction and metabolite identification from tandem mass spectra. Nucleic Acids Res. 2014;42(W1):W94–9. https://doi.org/10.1093/nar/gku436.
23. Yukihira D, Miura D, Saito K, Takahashi K, Wariishi H. MALDI −MS-based high-throughput metabolite analysis for intracellular metabolic dynamics. Anal Chem. 2010;82(10):4278–82. https://doi.org/10.1021/ac100024w.
24. Miura D, Fujimura Y, Tachibana H, Wariishi H. Highly sensitive matrix-assisted laser desorption ionization-mass spectrometry for high-throughput metabolic profiling. Anal Chem. 2010;82(2): 498–504. https://doi.org/10.1021/ac901083a.
25. Zhang Y, Wang Y, Guo S, Guo Y, Liu H, Li Z. Ammonia-treated N-(1-naphthyl) ethylenediamine dihydrochloride as a novel matrix for rapid quantitative and qualitative determination of serum free fatty acids by matrix-assisted laser desorption/ionization-Fourier transform ion cyclotron resonance mass spectrometry. Anal Chim Acta. 2013;794:82–9. https://doi.org/10.1016/j.aca.2013.07.060.
26. Chong J, Soufan O, Li C, Caraus I, Li S, Bourque G, et al. MetaboAnalyst 4.0: towards more transparent and integrative metabolomics analysis. Nucleic Acids Res. 2018; gky310-gky310.
27. Lu J, Idris U, Harmon B, Hofacre C, Maurer JJ, Lee MD. Diversity and succession of the intestinal bacterial Community of the Maturing Broiler Chicken. Appl Environ Microbiol. 2003;69(11): 6816–24. https://doi.org/10.1128/AEM.69.11.6816-6824.2003.
28. Scupham AJ. Succession in the intestinal microbiota of preadolescent turkeys. FEMS Microbiol Ecol. 2007;60(1):136–47. https://doi.org/10.1111/j.1574-6941.2006.00245.x.
29. Cheung Lam AH, Sandoval N, Wadhwa R, Gilkes J, Do TQ, Ernst W, et al. Assessment of free fatty acids and cholesteryl esters delivered in liposomes as novel class of antibiotic. BMC Res Notes. 2016;9(1):337. https://doi.org/10.1186/s13104-016-2138-8.
30. Zheng CJ, Yoo J-S, Lee T-G, Cho H-Y, Kim Y-H, Kim W-G. Fatty acid synthesis is a target for antibacterial activity of unsaturated fatty acids. FEBS Lett. 2005;579(23):5157–62. https://doi.org/10.1016/j.febslet.2005.08.028.
31. Crompton MJ, Dunstan RH, Macdonald MM, Gottfries J, von Eiff C, Roberts TK. Small changes in environmental parameters Lead to alterations in antibiotic resistance, cell morphology and membrane fatty acid composition in Staphylococcus lugdunensis. PLoS One. 2014;9(4):e92296.
32. Defez R, Esposito R, Angelini C, Bianco C. Overproduction of indole-3-acetic acid in free-living rhizobia induces transcriptional changes resembling those occurring in nodule Bacteroids. Mol Plant-Microbe Interact. 2016;29(6):484–95. https://doi.org/10.1094/MPMI-01-16-0010-R.
33. Matilla MA, Daddaoua A, Chini A, Morel B, Krell T. An auxin controls bacterial antibiotics production. Nucleic Acids Res. 2018; gky766-gky766.
34. Bianco C, Imperlini E, Calogero R, Senatore B, Pucci P, Defez R. Indole-3-acetic acid regulates the central metabolic pathways in Escherichia coli. Microbiology. 2006;152(8):2421–31.
35. Zelante T, Iannitti Rossana G, Cunha C, De Luca A, Giovannini G, Pieraccini G, et al. Tryptophan catabolites from microbiota engage aryl hydrocarbon receptor and balance mucosal reactivity via Interleukin-22. Immunity. 2013;39(2):372–85. https://doi.org/10.1016/j.immuni.2013.08.003.
36. Taub FE, DeLeo JM, Thompson EB. Sequential comparative hybridizations analyzed by computerized image processing can identify and quantitate regulated RNAs. DNA. 1983;2(4):309–27. https://doi.org/10.1089/dna.1983.2.309.
37. Pollack JR, Perou CM, Alizadeh AA, Eisen MB, Pergamenschikov A, Williams CF, et al. Genome-wide analysis of DNA copy-number changes using cDNA microarrays. Nat Genet. 1999;23:41.
38. Schäferling M. Methods in molecular biology Vol. 671: Biological microarrays: methods and protocols. Edited by Ali Khademhosseini, Kahp-Yang Suh and Mohammed Zourob. ChemBioChem. 2011;12(10):1602–3. https://doi.org/10.1002/cbic.201100279.
39. Hutchens TW, Yip T-T. New desorption strategies for the mass spectrometric analysis of macromolecules. Rapid Commun Mass Spectrom. 1993;7(7):576–80. https://doi.org/10.1002/rcm.1290070703.

Rebecca Hansen received her B.S. from University of Wisconsin-Platteville in 2013 and her Ph.D. degree in Analytical Chemistry under the supervision of Dr. Young Jin Lee at Iowa State University in 2018. Her Ph.D. research focused on MALDI-mass spectrometry imaging and high-throughput metabolomics.

Maria Emilia Dueñas completed her B.S. in Chemistry at Universidad San Francisco de Quito (Ecuador) in 2013. She is a Ph.D. candidate in Analytical Chemistry at Iowa State University under the supervision of Dr. Young Jin Lee. Her research has focused upon advancing the field of metabolomics using high-spatial resolution MALDI-mass spectrometry imaging.

Torey Looft is a research microbiologist at National Animal Disease Center, US Department of Agriculture-Agricultural Research Station. His research interests include characterization of poultry microbiomes, investigation of the effects of antibiotic feed additives on the expression and transmission of fitness, and antimicrobial resistance genes in intestinal microbial populations. He is also interested in the evaluation of environmental and host influences on gut bacterial ecological niches and foodborne pathogen control strategies.

Young Jin Lee is Associate Professor in the Department of Chemistry, Iowa State University. He has over 25 years of expertise in various areas of mass spectrometry. His current research interests include mass spectrometry imaging of small molecules, MALDI-MS-based high-throughput assay, and high-resolution MS of biomass pyrolysis. He is interested in applying these techniques to understand plant metabolism at the cellular level, chemical interactions in gut microbiome, and forensic chemical fingerprint analysis.